Santiago-Portillo, A.; Remiro-Buenamañana, S.; Navalón Oltra, S.; García Gómez, H. (2019). Subphthalocyanine encapsulated within MIL-101(Cr)-NH2 as a solar light photoredox catalyst for dehalogenation of alpha-haloacetophenones. Dalton Transactions. 48(48):17735-17740. https://doi.org/10.1039/c9dt04004h

ARTICLE

Subphthalocyanine encapsulated within in MIL-101(Cr)-NH_2 as solar light photoredox catalyst for dehalogenation of α-haloacetophenones

Received 00th January 20xx,
Accepted 00th January 20xx

DOI: 10.1039/x0xx00000x

Andrea Santiago-Portillo,[a] Sonia Remiro-Buenamañana,[b] Sergio Navalón,[a] Hermenegildo García[a,b,c*]

Subphthalocyanine has been incorporated into a robust metal-organic framework having amino groups as binding sites. The resulting SubPc@MIL-101(Cr)-NH_2 composite has a loading of 1 wt.%. Adsorption of subphthalocyanine does not deteriorate host crystallinity, but decreases the surface area and porosity of the MIL-101(Cr)-NH_2. The resulting SubPc@MIL-101(Cr)-NH_2 composite exhibits a 575 nm absorption band responsible for the observed photoredox catalytic activity under simulated sunlight irradiation for hydrogenative dehalogenation of α-haloacetophenones and for the coupling of α-bromoacetophenone and styrene. The material undergoes a slight deactivation upon reuse. In comparison to the case of phthalocyanines the present study is one of the few cases showing the use of subphthalocyanine as photoredox catalyst, activity deriving from site isolation within the MOF cavities.

Introduction

Metal-organic frameworks (MOFs) are currently among the most intensely studied photocatalysts due to the efficient photoinduced electron transfer from the excited linker to the metal nodes.[1-9] However, very frequently the organic linkers do not have photoresponse under visible light and different strategies have been developed to expand MOF photoresponse to the visible region. Among them, one that has been widely used is substitution of the aromatic linker with amino groups that introduce a new n → π* electronic transition with onset about 450 nm.[2] However, in most of the cases, amino group substitution does not expand the photoresponse towards the red beyond 450 nm. For this reason, alternative strategies consisting in the anchoring on peripheral framework positions of additional chromophores or metallic complexes such as ruthenium(II) polypyridyl complexes, has been also applied.[1, 2, 5] In this context, although MOFs with phthalocyanines units as organic linkers have been well-established as photocatalysts,[10] the use of subphthalocyanines have so far not been reported in spite of the intense absorption band that these macrocyclic dyes exhibit in the visible region.[11-13]

In the present study, the preparation of MIL-101(Cr)-NH_2 containing subphthalocyanine (SubPc@MIL-101(Cr)-NH_2) as visible light harvester unit will be described. This composite exhibits activity for the sunlight photoredox catalytic hydrogenative debromination of bromoacetophenone in the presence of electron donors (photoredox reaction).[14]

Results and discussion

Photocatalyst preparation and characterization

MIL-101(Cr)-NH_2 was selected in the present study as host of SubPc-Cl for various reasons, including framework robustness, the presence of -NH_2 as apical binding sites for SubPc-Cl, large porosity, high surface area and reliable synthesis.[15-17] The presence of amino groups on the terephthalate linkers are expected to act as binding sites for the apical position of SubPc-Cl, replacing Cl-.[18, 19] It is expected that substitution of Cl- in SubPc-Cl by amino groups located on the MOFs cavities would result on the formation of a strongly bound composite that could exhibit visible light photoresponse due to the optical properties of SubPc.[20-23] Scheme 1 illustrates the incorporation procedure and the anchoring of SubPc-Cl through the –NH_2 substituents.

[a] Departamento de Química, Universitat Politècnica de València, C/Camino de Vera, s/n, 46022, Valencia, Spain.
[b] Instituto Universitario de Tecnología Química, CSIC-UPV, Universitat Politécnica de Valencia, Av. de los Naranjos, Valencia 46022, Spain.
[c] Center of Excellence for Advanced Materials Research, King Abdulaziz University, Jeddah, Saudi Arabia.

Electronic Supplementary Information (ESI) available: Characterization and catalytic. See DOI: 10.1039/x0xx00000x

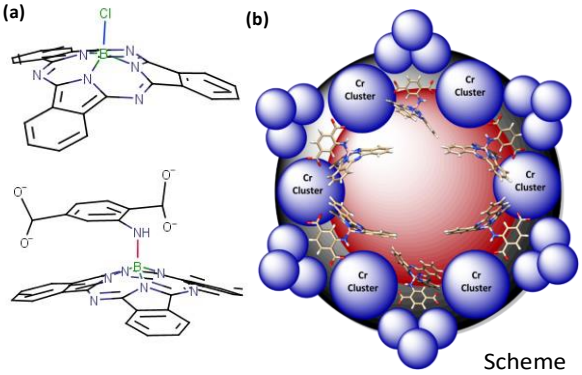

Scheme 1. a) Structure of SubPc-Cl and its covalent linkage (red bond) with the –NH_2 groups present in the therephthalate organic ligand of MIL-101(Cr)-NH_2; b) Cartoon illustrating the structure of SubPc@MIL-101(Cr)-NH_2 (red sphere: pore; blue spheres: Cr clusters; and black sphere: MIL101(Cr)-NH_2).

After incorporation of SubPc-Cl into MIL-101(Cr)-NH_2, isothermal gas adsorption measurements reveal a large decrease in the surface area value and a diminution of the porosity (Table 1).

The amount of SubPc adsorbed on MIL-101(Cr)-NH_2 was estimated by combustion elemental analysis of carbon and nitrogen and from comparison of the thermogravimetric profile of MIL-101(Cr)-NH_2 and SubPc@MIL-101(Cr)-NH_2. The data are also given in Table 1, while Figure S1 in supporting information show the thermogravimetric profiles of these two solids, where it can be seen that the percentage of residual weight after decomposition of the organic components is larger for SubPc@MIL-101(Cr)-NH_2 as compared to MIL-101(Cr)-NH_2. Analytical data indicates that the percentage of subphthalocyanine guest in the composite material corresponds to about 1 wt.%.

XRD of SubPc@MIL-101(Cr)-NH_2 is coincident with that of MIL-101(Cr)-NH_2, indicating that the crystal structure of the MOFs is preserved upon adsorption of SubPc-Cl. The absence of characteristic peaks corresponding to SubPc-Cl in the XRD of the SubPc@MIL-101(Cr)-NH_2 composite indicates that no crystals of the boron macrocycle are detectable in the guest, this being compatible with site isolation of individual SubPc macrocycles inside host cavities (Figure 1).

Table 1. Isothermal N_2 adsorption and relevant elemental analysis of MIL-101(Cr)-NH_2 and SubPc@MIL-101(Cr)-NH_2.

	MIL-101(Cr)-NH_2	**SubPc@MIL-101(Cr)-NH_2**
BET surface area ($m^2\ g^{-1}$)	1950	490
Pore volume ($cm^3\ g^{-1}$)	2	0.6
N (%)	3.2	4.9
C (%)	22.2	32.1

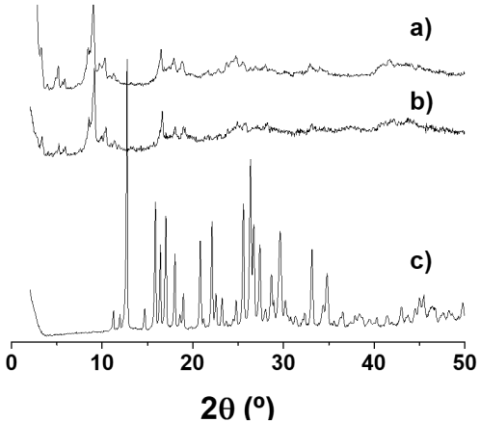

Figure 1. XRD patterns of a) MIL-101(Cr)-NH_2, b) SubPc@MIL-101(Cr)-NH_2 and c) SubPc-Cl.

The presence of SubPc as guests incorporated into MIL-101(Cr)-NH_2 can be assessed by diffuse reflectance UV-Vis absorption spectroscopy, where the presence of a new band with λ_{max} about 570 nm, attributable to the presence of SubPc can be observed. Figure 2 shows a comparison of the diffuse reflectance UV-Vis spectra of MIL-101(Cr)-NH_2 and that of the composite SubPc@MIL-101(Cr)-NH_2. Figure S2 shows the diffuse reflectance UV-Visible spectra of SubPc-Cl. Comparison on the visible band corresponding to occluded SubPc with that of the parent SubPc-Cl shows a clear red shift of the adsorption band from 495 to 575 nm. This notable shift can be attributed to the exchange as apical ligand of chloride by the aromatic amino group, in agreement with the success of the SubPc-Cl adsorption by strong interaction with the amino groups.

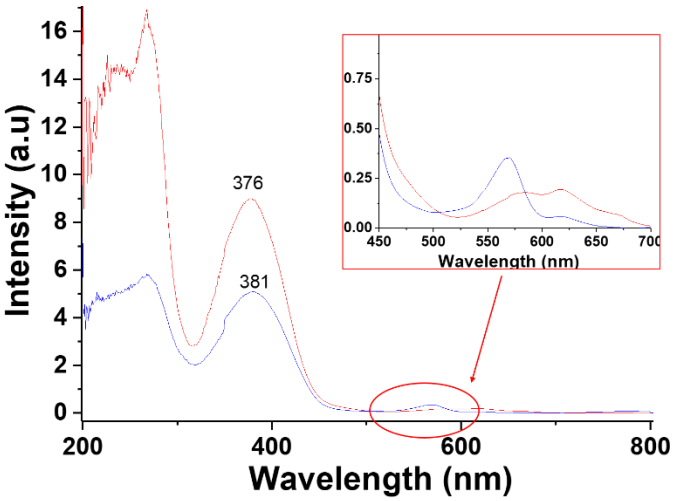

Figure 2. Diffuse reflectance UV-Vis spectra of MIL-101(Cr)-NH_2 (red line) and SubPc@MIL-101(Cr)-NH_2 (blue line).

Coincident conclusions can be achieved by analysis of the peaks corresponding to the different elements in XPS. Figure 3 summarizes the most characteristic data obtained by XPS, while

Figures S3-S5 in the supporting information provide additional information of the XPS peaks for each element. The most salient features from XPS analysis are the observation of additional signals for B 1s and Cl 2p present in the SubPc@MIL-101(Cr)-NH_2 composite respect to that of pristine MIL-101(Cr)-NH_2 host, indicating the presence of SubPc in the material. Interestingly, the B 1s peak is split into two individual components that can be attributed to B atoms interacting with amino groups of the linker and with Cl- anions. This interpretation agrees with the presence of Cl in the SubPc@MIL-101(Cr)-NH_2 composite, indicating that no complete replacement of apical Cl ligand by NH_2 has occurred during the adsorption.

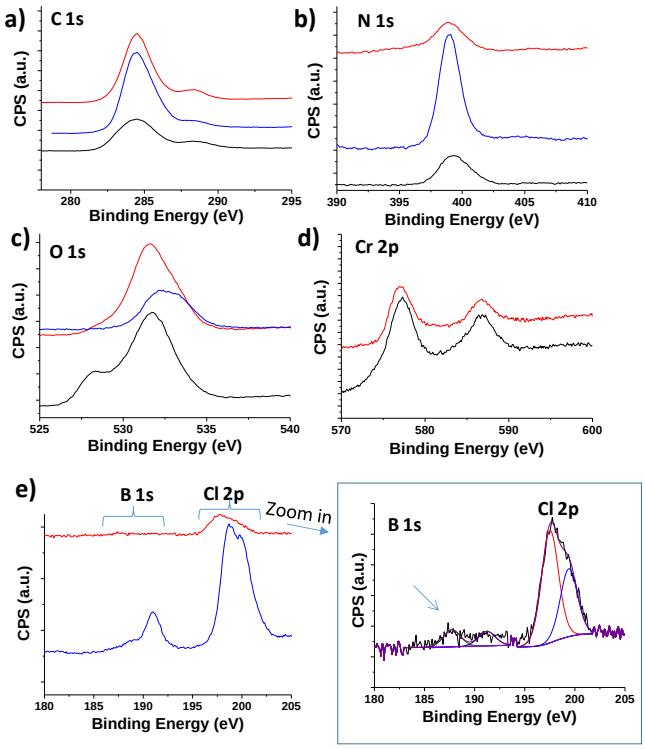

Figure 3. XPS spectra of MIL-101(Cr)-NH_2 (black line), SubPc@MIL-101(Cr)-NH_2 (red line) and SubPc-Cl (blue line).

As commented in the introduction, the purpose of this study was to show that adsorption of SubPc-Cl into MIL-101(Cr)-NH_2 as light harvesting centre affords a photoredox activity with enhanced visible light photoresponse for hydrogenative debromination of α-bromoacetophenone (Figure 4a).

Initial experiments were carried out with simulated sunlight in acetonitrile using triethanolamine (TEOA) as electron donor. The results of the photoredox test are presented in Figure 4. As it can be seen in this Figure, while negligible conversion is observed in the absence of any photocatalyst, the use of MIL-101(Cr)-NH_2 results only in a 15 % debromination at 8 h of irradiation. In contrast, using SubPc@MIL-101(Cr)-NH_2 as photoredox catalyst, a complete conversion of α-bromoacetophenone into acetophenone was achieved for this time. It should be noted that the reaction does not take place in the absence of visible light irradiation.

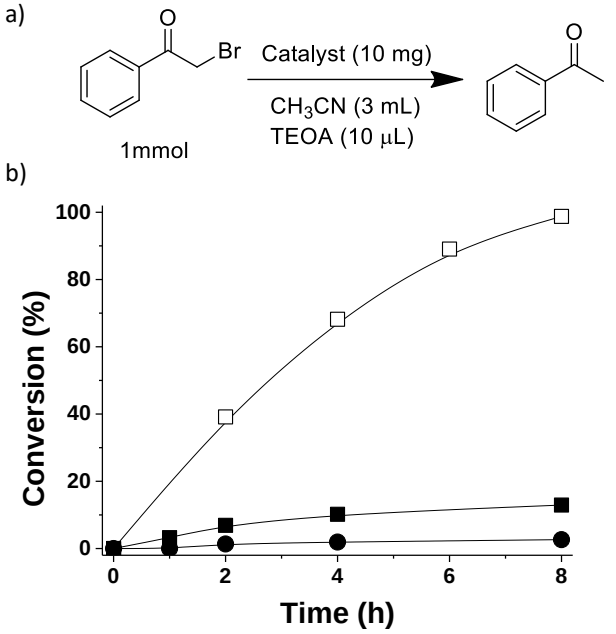

Figure 4. Time-conversion plot for the hydrogenative debromination of α-bromoacetophenone to acetophenone using (■) MIL-101(Cr)-NH_2, (□) SubPc@MIL-101(Cr)-NH_2 and (●) without any catalyst. Reaction conditions: α-bromoacetophenone (1 mmol), TEOA (10 μL), CH_3CN (3 mL) and MOF (10 mg, 0.35 mmol SubPc).

Photocatalytic stability of the composite was studied performing consecutive runs. Figure 5 shows the temporal profiles of the photoredox debromination activity upon reuse of the same SubPc@MIL-101(Cr)-NH_2 sample. The results show that the photoredox activity is maintained with only a slight decay from 90 to 83 % after 4 uses.

3.2. Photoredox catalysis

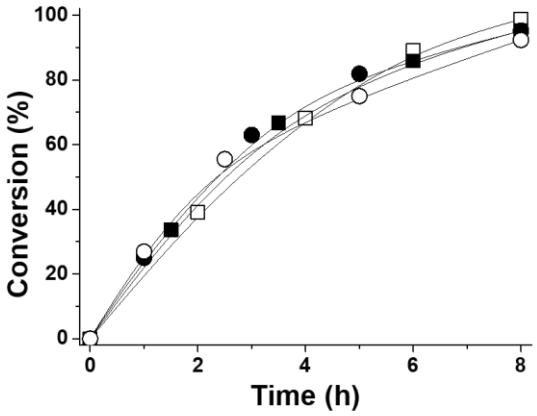

Figure 5. Time-conversion plot for the hydrogenative debromination of α-bromoacetophenone to acetophenone upon consecutive reuses using SubPc@MIL-101(Cr)-NH_2 as photoredox catalyst. Legend: (■) 1st use (□) 2nd use, (●) 3rd use and (○) 4th use. Reaction Conditions: α-bromoacetophenone (1 mmol), TEOA (10 µL), CH_3CN (3 mL) and MOF (10 mg, 0.35 mmol SubPc).

The SubPc@MIL-101(Cr)-NH_2 composite was also efficient to promote α-dechlorination of chloroacetophenone, although comparison of the temporal profiles of the bromo- and chloro-derivatives show that the reaction is slower in the case of α-chloroacetophenone, in accordance with the higher bond strength of C-Cl respect to C-Br. Figure S6 in the supporting information shows a comparison of the photocatalytic activity for dechlorination with respect to debromination.

The fact that the reaction mechanism involves the generation of the α-ketyl radical was confirmed by quenching of these radicals by 2,2,4,4-tetrametylpiperidinyloxy (TEMPO). Thus, if the photoredox debromination under simulated sunlight irradiation using SubPc@MIL-101(Cr)-NH_2 composite is started under the conventional reaction conditions and, then, after 2 h reaction, TEMPO is added to the reaction mixture no further progress in the formation of acetophenone is observed. Figure S7 compares the temporal profiles of the photocatalytic debromination in the absence and in the presence of TEMPO.
Finally, the solar light photoresponse of SubPc@MIL-101(Cr)-NH_2 was also applied for the photocatalytic coupling of α-bromoacetophenone and styrene to form α-phenylbutyrophenone, irradiating with simulated sunlight. In this photoredox reaction, the α-ketyl radical should add to the C=C double bond of styrene, since this vinylic substrate can easily undergo attack by radicals as previously reported.(Elisabeth Speckmeier, Patrick J. W. Fuchs and Kirsten Zeitler, A synergistic LUMO lowering strategy using Lewis acid catalysis in water to enable photoredox catalytic, functionalizing C–C cross-coupling of styrenes. Chem. Sci., 2018, 9, 7096–7103). It is

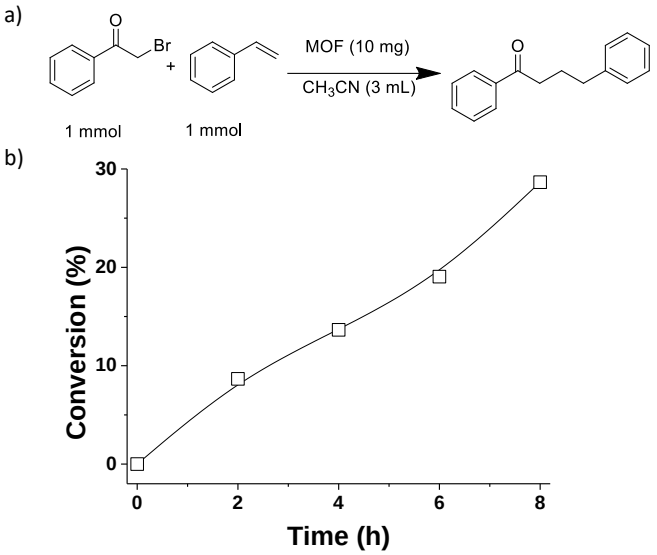

interesting to note that although conversion was not high, selectivity to α-phenylbutyrophenone was almost complete. It should be mention also in this case that the reaction does not occur in the absence of visible light irradiation. Figure 6 shows the temporal profile of butyrophenone formation.

Figure 6. Time-conversion plot for the coupling of α-bromoacetophenone and styrene using SubPc@MIL-101(Cr)-NH_2 as photoredox catalyst. Reaction conditions: α-bromoacetophenone (1 mmol), styrene (1 mmol), CH_3CN (3 mL) and MOF (10 mg, 0.35 mmol SubPc).

Experimental

Materials

All the reagents and solvents used in the present paper were of analytical or HPLC grade and supplied by Sigma-Aldrich.

Catalyst preparation

MIL-101(Cr)-NH_2 preparation. MIL-101(Cr)-NO_2 was prepared following already reported procedures.[16, 17] Briefly, nitroterephtalic acid (1.5 mmol) and $CrCl_3$ (1 mmol) were introduced into a Teflon autoclave containing demineralized water (8 mL). Then, the autoclave was heated at 180 ºC during 120 h. Once the autoclave was cooled at room temperature, the precipitate formed in the process was washed several times with dimethylformamide (DMF) at 120 ºC and, then, with ethanol at 80 ºC. Then, MIL-101(Cr)-NO_2 was submitted to a post-synthetic modification using $SnCl_2$·H2O as reducing agent leading to the formation of MIL-101(Cr)-NH_2 according to reported procedures.[16, 17]

SubPc@MIL101(Cr)-NH_2 preparation. Boron chloride subphthalocyanine (SubPc-Cl) was synthesized following reported literature procedures.[18, 24] Then, MIL101(Cr)-NH_2 (60 mg) was thermally activated by heating at 150 °C under vacuum in a 3 necked round bottomed flask connected to a reflux condenser during 22 h. SubPc-Cl (6 mg) was dissolved in dry

toluene (6 mL) and the solution was added to the flask containing the active MOF. The suspension was, then, refluxed under inert atmosphere for 48 h. The dispersion was filtered under vacuum and washed with toluene, the resulting solid was subsequently subjected to a Soxhlet extraction using chloroform (150 mL) as solvent until the extracts were colorless.

Catalyst characterization

Powder X-ray diffraction (PXRD) of the materials was recorded on a Philips XPert diffractometer equipped with a graphite monochromator (40 kV and 45 mA) employing Ni filtered CuKα radiation. N_2 adsorption isotherms at 77 K were recorded using a Micromeritics ASAP 2010 device. Thermogravimetric analyses were performed on a TGA/SDTA851e METTLER TOLEDO station. X-ray photoelectron spectra (XPS) of the different solids were collected on a SPECS spectrometer equipped with a MCD-9 detector using a monochromatic Al (K_α= 1486.6 eV) X-ray source calibrating the binding energy based on the the C 1s peak set at 284.4 eV as reference. CASA software has been employed for spectra deconvolution. Diffuse reflectance UV−visible spectra have been recorded using a Cary 5000 Varian spectrophotometer having an integrating sphere. (Sonia add experimental conditions for measurement)

Catalytic experiments

The required amount of catalyst (10 mg) was introduced into a quartz tube containing acetonitrile (3 mL) dissolved in α-bromoacetophenone (1 mmol) and TEOA (10 µL) and the system purged with Ar. Then, the tube was irradiated with a solar simulator. The reactions were magnetically stirred and reaction aliquots were sampled at the corresponding reaction times.

In the reusability experiments, the SubPc@MIL-101(Cr)-NH_2 solid was recovered at the end of the reaction by filtration (Nylon filter, 0.2 µm). Then, the catalyst was transferred to a round-bottom flask (50 mL) and submitted to ethanol washings (20 mL) under magnetic stirring for 30 min. This procedure was repeated two more times. The final solid was recovered by filtration (Nylon filter, 0.2 µm) and dried in an oven.

In the case of the coupling of α-bromoacetophenone and styrene, 10 mg of catalyst was mixed with 3 mL of acetonitrile containing 1 mmol of α-bromoacetophenone and 1 mmol of styrene using a quartz test tube and, the, the system purged with argon. Subsequently, the reaction tube was irradiated with a solar simulator. The reaction was magnetically stirred and reaction aliquots were sampled at the corresponding reaction times.

Product analysis

Previously filtered reaction aliquots were diluted in an acetonitrile solution containing a known amount of nitrobenzene as external standard. The aliquots were immediately analyzed by gas chromatography (GC) using a flame ionization detector. Quantification was carried out based on calibration plots obtained with authentic samples against nitrobenzene. Reaction products were identified using GC (Hewlett Packard HP6890 Chromatograph) coupled to a mass spectrometer (MS, Agilent 5973).

Conclusions

The present study shows that adsorption of subphthalocyanine at a loading of about 1 wt.% inside a robust MOF having amino groups in the terephthalate linker as binding sites renders a composite with solar light photoresponse that is able to promote hydrogenative debromination of α-haloacetophenones. The reaction involves ketyl radicals and the catalyst can be reused with only minor decay in photocatalytic activity. Since compared to related phthalocyanines, subphthalocyanines have been much less used as light harvesters and photosensitizers, the present study illustrates the potential that this boron macrocycle can have in photoredox catalysts.

Conflicts of interest

There are no conflicts to declare.

Acknowledgements

Financial support by the Spanish Ministry of Economy and Competitiveness (Severo Ochoa and RTI2018-098237-B-C21) and Generalitat Valenciana (Prometeo 2017-083) is gratefully acknowledged. S.N. thanks financial support by the Fundación Ramón Areces (XVIII Concurso Nacional para la Adjudicación de Ayudas a la Investigación en Ciencias de la Vida y de la Materia, 2016), Ministerio de Ciencia, Innovación y Universidades RTI 2018-099482-A-I00 project and Generalitat Valenciana grupos de investigación consolidables 2019 (ref: AICO/2019/214) project. S.R.-B. also thanks the Research Executive Agency (REA) and the European Commission, for the funding received under the Marie Skłodowska Curie actions (H2020-MSCA-IF-2015/ Grant agreement number 709023/ ZESMO).

Notes and references

1. X. Deng, Z. Li and H. García, *Chem. Eur. J.*, 2017, **23**, 11189-11209
2. A. Dhakshinamoorthy, A. M. Asiri and H. García, *Angew. Chem. Int. Ed.*, 2016, **55**, 5414-5445
3. D. Jiang, P. Xu, H. Wang, G. Zeng, D. Huang, M. Chen, C. Lai, C. Zhang, J. Wan and W. Xue, *Coord. Chem. Rev.*, 2018, **376**, 449-466
4. R. Li, W. Zhang and K. Zhou, *Adv. Mater.*, 2018, **30**, 1705512.
5. J. Qiu, X. Zhang, Y. Feng, X. Zhang, H. Wang and J. Yao, *Appl. Catal. B.-Env.*, 2018, **231**, 317-342
6. L. Shen, R. Liang and L. Wu, *Chin. J. Catal.*, 2015, **36**, 2071-2088
7. Y. Shi, A.-F. Yang, C.-S. Cao and B. Zhao, *Coord. Chem. Rev.*, 2019, **390**, 50-75
8. S. Wang and X. Wang, *Small*, 2015 **11**, 3097-3112
9. M. Wen, K. Mori, Y. Kuwahara, T. An and H. Yamashita, *Chem. Asian J.*, 2018, **13**, 1767-1779
10. S. Das and W. M. A. Wan Daud, *Renew. Sust. Energ. Rev.*, 2014, **39**, 765-805

11. B. del Rey, U. Keller, T. Torres, G. Rojo, F. Agulló-López, S. Nonell, C. Martí, S. Brasselet, I. Ledoux and J. Zyss, *J. Am. Chem. Soc.*, 1998, **120**, 12808-12817.
12. C. G. Claessens, D. González-Rodrí guez and T. Torres, *Chem. Rev.*, 2002, **102**, 835−853.
13. N. Kobayashi, In The Porphyrin Handbook, Kadish, K. M.; Smith, K. M.; Guilard, R., Eds. Academic Press: Amsterdam, 2003; pp 161-262., 2003.
14. A. Santiago-Portillo, H. G. Baldoví, E. Carbonell, S. Navalón, M. Alvaro, H. García and B. Ferrer, *J. Phys. Chem. C*, 2018, **122**, 29190-29199
15. G. Ferey, C. Mellot-Draznieks, C. Serre, F. Millange, J. Dutour, S. Surble and I. Margiolaki, *Science*, 2005, **309**, 2040-2042.
16. A. Santiago-Portillo, J. F. Blandez, S. Navalón, M. Álvaro and H. García, *Catal. Sci. Technol.,* 2017, **7**, 1351-1362.
17. A. Santiago-Portillo, S. Navalón, P. Concepción, M. Álvaro and H. García, *ChemCatChem*, 2017, **9**, 2506-2511
18. C. G. Claessens, D. Gonzalez-Rodriguez, M. S. Rodriguez-Morgade, A. Medina and T. Torres, *Chem. Rev.*, 2014, **114**, 2192 - 2277.
19. J. Guilleme, L. Martínez-Fernández, D. González-Rodríguez, I. Corral, M. Yáñez and T. Torres, *J. Am. Chem. Soc.*, 2014, **136**, 14289-14298.
20. M. Managa, J. Mack, D. Gonzalez-Lucas, S. Remiro-Buenamañana, C. Tshangana, A. N. Cammidge and T. Nyokong, *J. J Porphyr. Phthalocya.*, 2015, **20**, 1-20.
21. G. Bressan, A. N. Cammidge, G. A. Jones, I. A. Heisler, D. Gonzalez-Lucas, S. Remiro-Buenamañana and S. R. Meech, *J. Phys. Chem. A.*, 2019, **123**, 5724-5733.
22. G. E. Morse and T. P. Bender, *ACS Applied Materials & Interfaces*, 2012, **4**, 5055-5068.
23. K. L. Sampson, X. Jiang, E. Bukuroshi, A. Dovijarski, H. Raboui, T. P. Bender and K. M. Kadish, *J. Phys. Chem. A*, 2018, **122**, 4414-4424.
24. C. G. Claessens, D. Gonzalez-Rodriguez, B. del Ray, T. Torres, G. Mark, H.-P. Schuchmann, C. von Sonntag, J. G. MacDonald and R. S. Nohr, *Eur. J. Org. Chem.*, 2003, 2547 - 2551.

